THE JOURNAL OF PHYSICAL CHEMISTRY C

Article

pubs.acs.org/JPCC

Postadsorption Work Function Tuning via Hydrogen Pressure Control

Hermann Edlbauer, Egbert Zojer, and Oliver T. Hofmann*

Institute for Solid State Physics, NAWI Graz, Graz University of Technology, 8010 Graz, Austria

Supporting Information

ABSTRACT: The work function of metal substrates can be easily tuned, for instance, by adsorbing layers of molecular electron donors and acceptors. In this work, we discuss the possibility of changing the donor/acceptor mixing ratio reversibly *after* adsorption by choosing a donor/acceptor pair that is coupled via a redox reaction and that is in equilibrium with a surrounding gas phase. We discuss such a situation for the example of tetrafluoro-1,4-benzenediol (TFBD)/tetrafluoro-1,4-benzoquinone (TFBQ), adsorbed on Cu(111) and Ag(111) surfaces. We use density functional theory and *ab initio* thermodynamics to show that arbitrary TFBD/TFBQ mixing ratios can be set using hydrogen pressures attainable in low to ultrahigh vacuum. Adjusting the mixing ratio allows modifying the work function over a range of about 1 eV. Finally, we contrast single-species submonolayers with mixed layers to discuss why the resulting inhomogeneities in the electrostatic energy above the surface have different impacts on the interfacial level alignment and the work function.

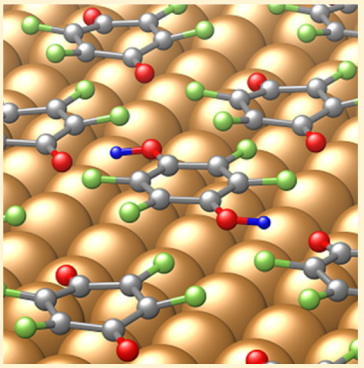

1. INTRODUCTION

For many applications, ranging from catalysis to electronics, the work function (Φ) of metals plays an important role. Particular interest comes from the field of organic electronics, where the performance of the devices is strongly affected by charge injection barriers built up at the interfaces between the metal electrodes and the organic semiconducters.[1] The electron and hole injection barriers, which exponentially affect the current density,[2] are (among other factors)[3] determined by the offset between the substrate Fermi energy and the charge-transport levels of the organic material that are typically associated with the lowest unoccupied and highest occupied molecular orbitals (LUMO and HOMO). A reduction of those barriers can be accomplished by adjusting Φ such that the Fermi level of the metal matches one of the charge-transport levels.[1] To this aim, several strategies have been developed, including the deposition of thin layers of alkali halides,[4−6] alkali/alkaline earth metals,[7,8] ultrathin oxide films,[9,10] or dipolar self-assembled monolayers.[11−16] Another particularly promising approach is the deposition of organic molecules undergoing charge-transfer reactions.[17,18] This bears the advantage of allowing for continuous Φ-tuning by varying the coverage of the adsorbed organic (sub)monolayer.[19,20] Upon employing this approach in organic light-emitting diodes, lower operating voltages as well as significant enhancements of electroluminescence and power efficiency were reported.[21]

Nonetheless, Φ-modification through coverage control faces certain practical problems: Often, the relation between work function and coverage is nonlinear,[20,22] and in some cases even abrupt changes of the work function with the molecular dosage have been reported.[23] Another complication arises from the observation that various molecules cannot be readily thermally desorbed from surfaces.[24,25] Thus, once a certain coverage is exceeded, a subsequent reduction is hardly possible. Furthermore, growth kinetics sometimes cause island[21] or needle[26] formation potentially leading to a nonuniform work function of the substrate. One possibility to restore the homogeneity of the surface is to use mixed monolayers containing two different molecular species with electron donor and acceptor character, respectively.[27,28] Here, we propose expanding this concept by choosing a donor/acceptor pair that is chemically "coupled", for example through a reaction with another gaseous (or liquid) substance. The particular advantage of this approach is that for such material combinations it would be possible to efficiently adjust the donor/acceptor mixing ratio after film deposition via the chemical potential (i.e., the partial pressure) of the reactant.[29]

A particularly well-suited class of materials for the aforementioned approach are acenequinones, which can react with hydrogen to acenediols (cf. Scheme 1).[30] Driven by a

Scheme 1. Reduction of Tetrafluoro-1,4-benzoquinone (TFBQ) with Molecular Hydrogen to Tetrafluoro-1,4-benzenediol (TFBD)

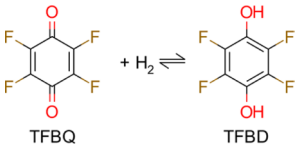

Received: September 10, 2015
Revised: November 6, 2015
Published: November 9, 2015

DOI: 10.1021/acs.jpcc.5b08827
J. Phys. Chem. C 2015, 119, 27162−27172

quinoid-to-aromat transition, acenequinones are strong electron acceptors,[31] whose deposition on the coinage metal surface yields pronounced work function increases.[32] In contrast, dioles are more electron rich, and one can expect them to lower the work function of a metallic substrate. A surrounding gas phase of hydrogen molecules allows controlling the diol vs quinone fraction, f, which is, thus, anticipated to act as an efficient handle for substantially increasing or decreasing the net substrate work function.

In this work we employ density functional theory to study the example of tetrafluoro-1,4-benzoquinone (TFBQ) and tetrafluoro-1,4-benzenediol (TFBD) as a model for an electron-acceptor and -donor pair and consider their adsorption on Cu(111) and Ag(111) surfaces. The chemical structures and the corresponding reaction with hydrogen are shown in Scheme 1. These systems are potentially not ideal for actual device applications, as due to their low molecular weight, diffusion into subsequently deposited organic semiconductor surfaces cannot be excluded (in practice, larger acenequinones, such as pentacenequinone or pentaceneteraone, will be better suited). Nevertheless, they are ideal systems for a proof of principles study, as (i) they are still fully suitable for portraying the general concept of a redox-coupled donor−acceptor pair (i.e., acenequinone/acenediol) and (ii) their comparably small size makes the necessary calculation of supercells containing several molecules computationally tractable.

The discussion is organized as follows: We start by investigating the adsorption properties of homogeneous monolayers of TFBQ and TFBD at full coverage. Employing *ab initio* thermodynamics, we then connect the hydrogen pressure in a surrounding gas phase, p_{H2}, to the fraction of reduced molecules, f, in a TFBQ monolayer. We show that at temperatures between 300 and 450 K arbitrary f can be achieved using technically feasible pressures of H_2, yielding work-function modifications over an energy range of about 1 eV. When comparing these work-function changes induced at varying coverages with those of mixed monolayers, we find fundamental differences that can be explained as a consequence of lateral inhomogeneity of the interfacial potential landscape.

2. THEORETICAL METHODS

Computational Details. Density functional theory (DFT) calculations were performed using the Fritz-Haber-Institute *ab initio* molecular simulations (FHI-aims) code.[33] We employed the Perdew−Burke−Ernzerhof[34] (PBE) exchange-correlation functional,[35] augmented by the vdW^{surf} method[36,37] to account for missing long-range van der Waals interactions. Previous investigations for charge-transfer molecules on metal surfaces showed that PBE+vdW^{surf} gives work-function modifications in good agreement with experiments, while hybrid functionals yield only minor or no improvements[38] despite the considerable increase of the computational effort.

Note that vdW^{surf} is an a posteriori correction that neglects the impact of van der Waals interactions on the electronic structure. Including these effects self-consistently[39] yields small changes of the work function of pristine Cu but has a stronger impact on Ag. To estimate the impact on our systems, we calculated the homogeneous layers of TFBQ and TFBD on both Cu and Ag using the self-consistent vdW^{surf} method. We find that the adsorption-induced work-function modification on Cu remains almost constant. On Ag, as for the pristine surface, the changes are more pronounced, and the work-function modification shifts by approximately 0.15 eV for both molecules. However, the range of the work-function modification covered by converting TFBQ into TFBD changes by less than 10%, and the conclusions drawn in this work are not affected by the specific treatment of dispersion forces.

The interface was modeled via the repeated slab approach with a four-layer slab of Cu(111) or Ag(111), separated from its periodic replicas in z-direction by at least 30 Å of vacuum. Additionally, a self-consistent dipole correction[40] was used to electrostatically decouple the slabs. The convergence of the energies for the thermodynamic model was verified against additional calculations containing six layers of metal. For each structure a geometry optimization was performed, constraining the bottom two metal layers and relaxing all other atoms until all remaining forces were smaller than 0.03 eV/Å. The lattice constants a for Cu (a_{Cu} = 3.632 Å) and Ag (a_{Ag} = 4.151 Å) were determined separately by maximizing the cohesive energy of the bulk crystal from a series of DFT calculations with variable a. The obtained lattice constants are in good agreement with both previous calculations based on a plane wave basis set[41] (a_{Cu} = 3.635 Å; a_{Ag} = 4.147 Å) and experiment (a_{Cu} = 3.603 Å; a_{Ag} = 4.069 Å, also taken from ref 41).

The repeated slab calculations with a single molecule in the two-dimensional unit cell were performed using a 12 × 12 × 1 Monkhorst−Pack k-point grid.[42] For larger cells the grid was scaled appropriately. The "tight" defaults, as shipped with FHI-aims, were used throughout all calculations, except for details of the confining potential of the numerically tabulated basis functions; the confining potential ensures a smooth decay of the wave functions to zero, and here we set the onset and width parameters to 4.6 and 2.6 Å, respectively, in order to increase the accuracy of the results.

For homogeneous layers of TFBQ and TFBD adsorbed on the metal surfaces, vibrations were calculated numerically at the Γ-point for the molecules in their respective unit cell. Numerical frequency evaluations require displacing each atom in the cell separately in each direction and evaluating the forces acting on these geometries. In this work, only atoms of the molecule were considered; the metal slab was kept fixed in order to keep the computational effort tractable. The displacement was set to 0.0025 Å, and evaluation of the forces acting on the atoms was set to 10^{-4} eV/Å.

Unit Cells. We assumed $(3 \times 3\sqrt{3})$ and $(\sqrt{7} \times \sqrt{7})$R18.1° surface unit cells for a single molecule on Cu(111) and Ag(111), respectively. These choices were inspired by LEED and STM experiments on hydroquinone (benzene-1,4-diol) adsorbed on Pt(111),[43] Pd(111),[44] and Rh(111)[45] and were corroborated by comparing their DFT total energies against various other plausible structures (for more details see Supporting Information). Moreover, we carefully tested several translations and rotations of the molecule after adsorption but found that the molecule always relaxes to a structure with the oxygen atoms in an "on-top" position, as shown in Figure 1 and explained in more detail in the Results section.

Different unit cells for Cu and Ag had to be chosen due to the differences in the metal lattice constants. These necessitated different alignments of the molecules to obtain comparable packing densities (the unit cell area per molecule is approximately 51 Å^2 on Cu and 52 Å^2 on Ag).

Supercells. Mixed monolayers of TFBQ and TFBD were modeled in (2 × 2) supercells on Cu(111) and Ag(111). These supercells contain four adsorption sites onto which the appropriate number of TFBQ and TFBD molecules was distributed. Two exemplary supercell geometries are shown in

DOI: 10.1021/acs.jpcc.5b08827
J. Phys. Chem. C 2015, 119, 27162−27172

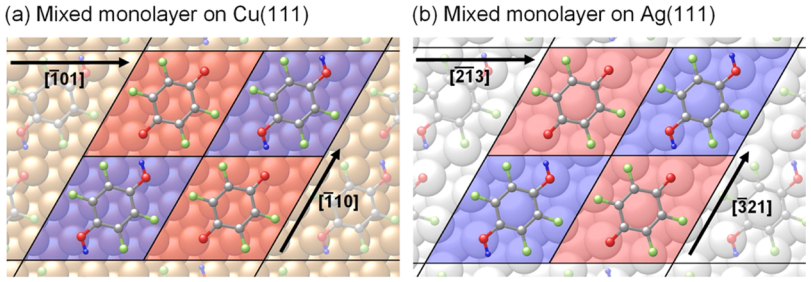

Figure 1. Exemplary 2 × 2 supercell geometries with f = 50% of TFBQ and TFBD arranged in checkerboard pattern (a) on Cu(111) (four ($3 \times 3\sqrt{3}$) cells in the supercell) and (b) on Ag(111) (four ($\sqrt{7} \times \sqrt{7}$)R18.1° cells in the supercell).

Figure 1. For the supercell geometries different molecular orientations, alignments of the OH groups, and TFBD/TFBQ patterns were tested to determine the optimal, minimum energy structure (details are given in the Supporting Information). The resulting ground state energies were used as input for the thermodynamic model.

***Ab Initio* Thermodynamics.** An interface of a solid and a surrounding gas phase, modeled as an isothermal−isobaric ensemble, strives to minimize the excess Gibbs free energy per area, γ, of the system.[46−48] Here we consider the situation for the adsorption of H_2 on a full monolayer of TFBQ, bound to the respective metal. We implicitly assume that hydrogen preferentially adsorbs on the TFBQ molecules (rather than on the metal), forming TFBD in the process. To corroborate this assumption, we have compared the total energy of TFBD at 25% coverage with the coexistence of TFBQ and physisorbed and chemisorbed H_2 at the surface. In these tests, we find that the reaction of H_2 with TFBQ to TFBD is at least 1.4 eV more favorable than the adsorption of hydrogen (dissociated or not) on the metal surface.

The organic molecules and the metal are treated jointly as the solid phase, assuming a fixed packing density (i.e., no desorption of organic material is considered). In thermodynamic equilibrium, the diol fraction, f, will assume the value that minimizes γ at a given temperature T and for a given hydrogen pressure p. For every f, γ is then given as

$$\gamma = \frac{1}{A}(E_{sys} - E_{solid} - \mu_{H2}N_{H2} + p{\cdot}V - TS_{conf} + F_{vib}) \quad (1)$$

Here A is the area of the investigated supercell. E_{sys} is the ground state energy of the entire system after adsorption, i.e., the metal covered with a mixed TFBQ/TFBD layer. E_{solid} denotes the ground state energy prior to adsorption of H_2, i.e., the energy of a homogeneously TFBQ-covered surface. μ_{H2} is the chemical potential and N_{H2} the number of hydrogen molecules in the supercell that react with the TFBQ-covered metal surface. The reaction of TFBQ with a single hydrogen atom yields a radical species, which is highly reactive and unstable. Therefore, we always consider the complete reduction from TFBQ to TFBD (see Scheme 1). As a consequence of that and because our supercells always contain exactly four molecules, N_{H2} can be related to f via $f = N_{H2}/4$. The mechanical work term given by the product of total pressure, p, and volume, V, can be safely neglected.[46] S_{conf} denotes the configurational entropy of the mixed monolayer adsorbate. An upper estimate of this term can be provided by assuming that for a given f all conformations are degenerate. S_{conf} is then simply proportional to the *logarithmus naturalis* of the number of possible configurations. This is largest for f = 50%, where S_{conf} takes a maximum value of approximately 1.2×10^{-6} eV/(K A^2), prompting us to neglect this contribution.

F_{vib} describes the change in the vibrational free energy upon adsorption. This term is commonly neglected in the literature, mostly due to the high computational effort required to obtain it. However, it cannot be completely ignored here since by inducing a quinone-to-aromat transition the adsorption of hydrogen changes the chemical nature of all bonds of the adsorbate. Conversely, the impact of the nature of the molecules in neighboring unit cells on the vibrations can be expected to be comparatively small. Thus, we calculated the vibrational free energy only for homogeneously TFBQ and TFBD covered surfaces (and H_2) and used those values to calculate the change in the vibrational free energy per reduced molecule

$$\Delta F_{vib} = F_{vib}/f = F_{vib}^{TFBD,ads} - F_{vib}^{TFBQ,ads} - F_{vib}^{H2} \quad (2)$$

We find that already the zero-point energy shifts the energy balance by approximately 0.43 eV (0.38 eV) for adsorption on Cu (Ag) in favor of the quinone species; including the temperature dependence, i.e., occupying the vibrations according to Bose−Einstein statistics, has only a comparatively minor impact.

For a constant packing density of the monolayer, the term E_{solid} is constant and yields only an energy offset that can be neglected when studying the relative stability of different TFBD/TFBQ mixing ratios. Thus, eq 1 can be rewritten as

$$\gamma = \frac{1}{A}(E_{sys} - f(\mu_{H2}N_{TFBQ} - \Delta F_{vib})) + \text{const} \quad (3)$$

Treating H_2 as an ideal gas, the chemical potential is related to p_{H2} and T via[49]

$$\mu_{H2} = \varepsilon_{H2} + k_B T \ln\left(\frac{p_{H2}\lambda_{H2}(T)^3}{k_B T}\right) \quad (4)$$

with ε_{H2} being the ground state energy of a hydrogen molecule, k_B the Boltzmann constant, and λ_{H2} the thermal de Broglie wavelength of H_2. The latter is given as[50]

$$\lambda_{H2}(T) = h(2\pi m_{H2}k_B T)^{-1/2} \quad (5)$$

The symbols m_{H2} and h indicate the molecular mass of the hydrogen molecule and Planck's constant.

To obtain the phase diagram, we generated a variety of surface structures for each f with different molecular configurations and orientations. A comprehensive list of all structures investigated can be found in the Supporting Information. For each of the structures, $\gamma(p, T)$ is evaluated. Finally, the fraction of reduced molecules, f, for the

DOI: 10.1021/acs.jpcc.5b08827
J. Phys. Chem. C 2015, 119, 27162−27172

configuration minimizing γ at a given condition (p, T) is reported in the phase diagram (see below).

3. RESULTS AND DISCUSSION

Properties of Homogeneous Monolayers. Before we start focusing on the conversion of TFBQ to TFBD and the impact of the resulting mixed layers on the substrate, it is instructive to briefly review the properties of the limiting cases, where the surface is fully covered by either only the acceptor or the donor molecules.

For both metal substrates, TFBD remains planar and adsorbs at a distance of approximately 3.1 Å (see Table 1). On Cu (Ag) the adsorption distance of TFBQ is about 0.7 Å (0.3 Å) smaller than for TFBD (see Table 1). The observation that the adsorption distance of the carbonyl-containing molecule is smaller on Cu than on Ag is in line with the experimental observation for PTCDA on the same surfaces.[51] Furthermore, the planar structure of TFBQ is significantly distorted upon adsorption: On both substrates, the oxygen atoms are located below the carbon backbone, which is indicative of the formation of a bond between the carboxyl groups and the metal surface. This bonding leads to a small, partial extraction of surface metal atoms, which is discussed in the Supporting Information. Furthermore, on copper the fluorine atoms are located above the carbon backbone. A qualitatively similar distortion has previously been reported for the adsorption of perfluoropentacene based on X-ray standing wave experiments.[52] A summary of the adsorption distances of the different atomic species relative to the uppermost metal layer for the different adsorption cases can be found in Table 1, and the geometries are depicted in Figure 2.

Table 1. Adsorption Distances, d_X, of the Atomic Species, $X \in \{H,C,O,F\}$, Relative to the Relaxed Uppermost Metal Layer and Adsorption Energies, E_{ads}, for Homogeneous Monolayers of TFBQ and TFBD on Cu(111) and Ag(111) at Full Coverage[a]

adsorbate	surface	d_H [Å]	d_C [Å]	d_O [Å]	d_F [Å]	E_{ads} [eV]
TFBD	Cu(111)	2.89	3.03	3.06	3.07	−0.9
TFBD	Ag(111)	2.86	3.09	3.05	3.12	−0.9
TFBQ	Cu(111)	-	2.30	2.10	2.60	−2.6
TFBQ	Ag(111)	-	2.83	2.46	2.85	−1.5

[a]On Ag the topmost metal layer relaxed inward by 4 and 5 pm for adsorption of TFBD and TFBQ, respectively; for Cu the shifts are smaller than 1 pm.

We find that the adsorption energy, E_{ads}, differs strongly between the two molecular species (Table 1). Here, E_{ads} is defined as

$$E_{ads} = E_{sys} - E_{fsm} - E_{slab} \quad (6)$$

with the energy of the full system, E_{sys}, and the energies of the subsystems: the hypothetical, free-standing molecular monolayer, E_{fsm}, and the metal slab, E_{slab}. To obtain those, both slab and monolayer geometries are fixed at the structures of the combined system. For TFBQ E_{ads} is much larger than for TFBD. This agrees with the observation that also the geometric distortion is much larger for TFBQ, indicating that the metal surface forms a strong bond to the TFBQ species but not to the TFBD molecule.

The adsorption of a homogeneous monolayer of TFBD yields a decrease of Φ by −0.4 eV on Cu(111) and −0.3 eV on Ag(111); conversely, for homogeneous monolayers of TFBQ an increase of +0.5 eV on Cu and +0.6 eV on Ag is observed. $\Delta\Phi$ is commonly decomposed into three contributions: (i) a work-function shift due to the dipoles of the molecules in a hypothetical free-standing molecular monolayer (ΔE_{mol}) in the (distorted) geometry of the adsorbate; (ii) an equivalent work-function shift due to the asymmetry of the metal slab (ΔE_{slab}) arising from the relaxation of the metal surface below the molecules; and (iii) the bond dipole (ΔE_{bond}) resulting from charge rearrangements upon adsorption, i.e., from the metal−molecule bond formation

$$\Delta\Phi = \Delta E_{mol} + \Delta E_{slab} + \Delta E_{bond} \quad (7)$$

In principle, ΔE_{bond} can then be either calculated from the aforementioned charge rearrangements applying Poisson's equation or (equivalently) simply by subtracting ΔE_{mol} and ΔE_{slab} from $\Delta\Phi$. For the investigated system the values of ΔE_{slab} are smaller than 0.04 eV and thus are neglected in the following discussion.

Despite the strong geometrical distortion of TFBQ upon adsorption on Cu(111) no net molecular dipole exists (cf. Table 2) since the contributions of the electronegative F and O

Table 2. $\Delta\Phi$ and Its Contributions, ΔE_{mol} and ΔE_{bond}, for Adsorption of Homogeneous Monolayers of TFBQ and TFBD on Cu and Ag

adsorbate	surface	$\Delta\Phi$ [eV]	ΔE_{mol} [eV]	ΔE_{bond} [eV]
TFBD	Cu(111)	−0.4	+0.3	−0.7
TFBD	Ag(111)	−0.3	+0.3	−0.6
TFBQ	Cu(111)	+0.5	+0.0	+0.5
TFBQ	Ag(111)	+0.6	−0.5	+1.1

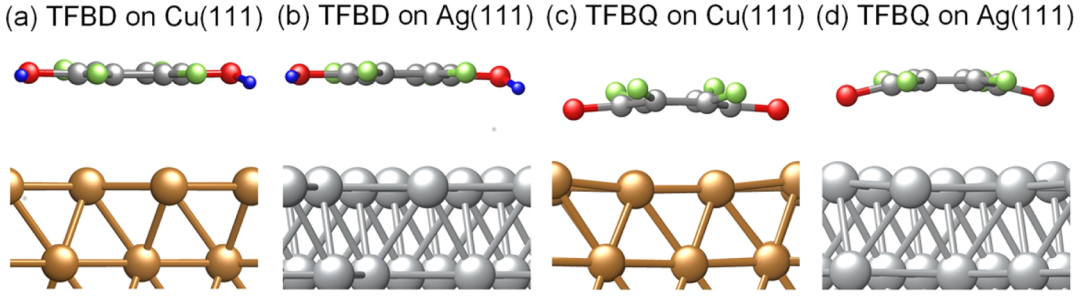

Figure 2. Adsorption geometries of homogeneous monolayers of (a) TFBD on Cu(111), (b) TFBD on Ag(111), (c) TFBQ on Cu(111), and (d) TFBQ on Ag(111). Note that the different apparent numbers of metal atoms originate from the different viewing angles due to the different orientations of the molecules on Cu and Ag (cf. Figure 1).

DOI: 10.1021/acs.jpcc.5b08827
J. Phys. Chem. C 2015, 119, 27162−27172

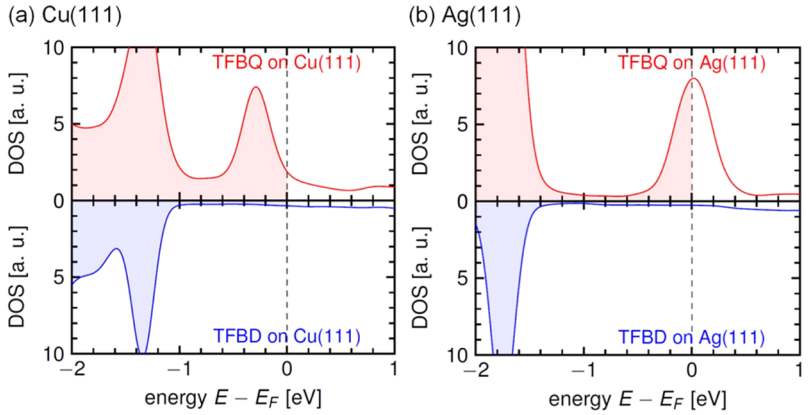

Figure 3. Density of states (DOS) for homogeneous monolayers of TFBQ (red) and TFBD (blue) adsorbed on (a) Cu(111) and (b) Ag(111).

atoms located above and below the electropositive carbon atoms cancel. Therefore, for TFBQ on Cu(111) $\Delta\Phi$ arises exclusively from the bond dipole. On Ag(111), the fluorine atoms remain within the plane of the carbon backbone. As a consequence, due to the appreciable downward bending of the oxygen atoms a large molecular dipole decreasing Φ is present.

For the adsorption of TFBD the negative contribution from the bond dipole dominates the work-function change: In the density of states of the adsorbed molecule shown in Figure 3 no peak is present at or close to E_F. This indicates the absence of charge transfer from or to molecular frontier orbitals. Also no indication for covalent bond formation can be found. Therefore, the occurrence of a bond dipole (cf. Table 2), that still renders the molecule formally positive, is assigned to Pauli pushback[53,54] (also known as cushion effect). In other words, the electron density above the copper surface that spills out into the vacuum is displaced by the adsorbate. Here, this causes relatively large values for ΔE_{bond} of −0.7 eV on Cu and −0.6 eV on Ag, which agree nicely with the work-function reductions observed for the deposition of inert alkanes on the same substrate surfaces.[55] On both Cu and Ag the Pauli pushback effect is mitigated by an opposing molecular dipole ΔE_{mol} of 0.3 eV, which results from one of the hydrogen atoms being located below the carbon backbone (for reasons that will be discussed below).

For TFBQ the large bond dipoles increasing Φ can be traced back to charge transfer from the substrate, which is caused by the high electron affinity (EA) of the molecule: In the Schottky−Mott limit the high EA would cause the lowest unoccupied molecular orbital (LUMO) of the hypothetically, free-standing TFBQ monolayer to lie below the Fermi energy. Such a situation is thermodynamically not stable and triggers electron transfer from the substrate to the adsorbate layer. For a homogeneous and dense packing the charged molecular layer and its counter charge are often thought to act akin to a plate capacitor,[1,11,56] inducing a shift in the electrostatic energy which increases the energy of the LUMO until it is in resonance with the Fermi level of the metal.[38] This effect, known as Fermi-level pinning, results in a fractional occupation of the DFT-LUMO as shown in Figure 3. To quantify the LUMO filling, we projected the density of states onto each of the molecular orbitals (shown in more detail in the Supporting Information). The occupation was then obtained by integrating the LUMO between $-\infty$ and E_F. We find that the metal donates 1.6 e^- on Cu and 0.9 e^- on Ag to the TFBQ LUMO. Interestingly, ΔE_{bond} shows the opposite trend and is twice as large on Ag as on Cu. The solution to this apparent conundrum is a strong hybridization of the carboxyl groups with the metal. This reduces the net occupation of deeper-lying occupied molecular orbitals. Such an interplay of charge donation and back-donation resembles the situation of the chemically similar molecule PTCDA on Cu and Ag[57] and is commonly observed for acenequinone molecules on coinage metal surfaces.[32] In the present case, this yields an observed net charge transfer of 0.17 e^- per molecule on Cu and 0.26 e^- on Ag. Together with the larger adsorption distance on Ag, this explains the *a priori* unexpected relation between the LUMO filling and ΔE_{bond}.

Mixed Monolayers and Hydrogen Pressure Dependence. Having understood the properties of the homogeneous monolayers, it is useful to clarify to which extent the fraction of the electron-donating molecules, f, in a mixed monolayer containing TFBQ and TFBD can be tuned by means of the hydrogen partial pressure, p_{H2}. The specific configuration, i.e., the mixing ratio between work-function increasing TFBQ and work-function reducing TFBD molecules in thermodynamic equilibrium at a given hydrogen pressure and temperature, is determined by the minimum of the Gibbs free energy per area, γ, for that situation. For each mixing ratio, we sampled a variety of different adsorption motifs and molecular arrangements. A top view of all investigated structures is provided in the Supporting Information.

When discussing the phase diagram of the organic adsorbate, particular attention needs to be paid to the potential existence of conformations that are energetically very close to the ground state. This situation is particularly common in systems that show cis−trans isomery or hindered rotations.[58,59] Here, this could apply to phases containing TFBD molecules. However, since each TFBD molecule can form up to two hydrogen bonds, the ground state energy depends very sensitively on the orientation of the hydroxyl groups. Each hydrogen atom may be located either on the "left" or on the "right" side of the molecule, giving rise to either a sickle-shaped molecule (if both are on the same side) or an S-shaped structure (if both are on opposite sides). Which of these structures is more stable depends on the nearest neighbor in the $[\bar{1}01]$-direction for Cu(111) or in the $[\bar{2}\bar{1}3]$ direction for Ag(111) (cf. indicated directions in Figure 1): When the next neighbor along this direction is again a TFBD molecule, both assume a sickle-shape structure. This allows one hydrogen to interact with the fluorine atom of the next neighbor (O−H···F) in the $[\bar{1}10]$-direction for Cu(111) or the $[\bar{3}21]$ direction for Ag(111) regardless whether this is a TFBQ or a TFBD molecule. The

DOI: 10.1021/acs.jpcc.5b08827
J. Phys. Chem. C 2015, 119, 27162−27172

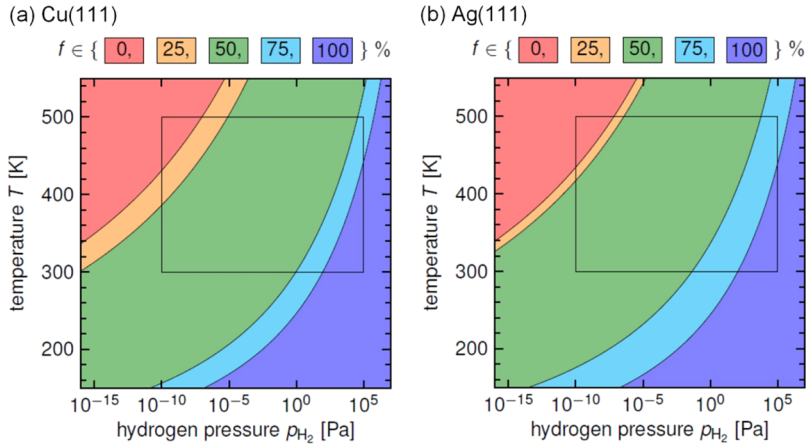

Figure 4. TFBD/TFBQ ratio f at thermodynamic equilibrium as a function of temperature and hydrogen pressure for mixed monolayers (a) on Cu(111) and (b) on Ag(111). The colors red, orange, green, cyan, and blue correspond to the TFBD fractions $f \in \{0, 25, 50, 75, 100\}$%. The box indicates the pressure range from ultrahigh to low vacuum and the temperature range from 300 to 500 K.

O−H···F motif always causes the hydrogen to lie between the metal and the carbon backbone, which is the reason why this molecule shows a small, but notable, permanent dipole perpendicular to the surface. (Noteworthy, this motif prevails if the fluorine atom is replaced by another hydrogen atom. Also, no geometry where the hydrogen is located above the carbon backbone is found to be stable.)

The other H forms a hydrogen bond with the O atom (O−H···O) of the TFBD molecule in the $[\bar{1}01]$-direction for Cu(111) or the $[\bar{2}\bar{1}3]$ direction for Ag(111). If one of these molecules would exhibit an S-shaped structure, the O−H···O bond could not form since the two hydrogen bonds would sterically hinder each other. In contrast, when the next neighbor in this direction is a TFBQ molecule, such a steric hindrance does not exist. This allows the TFBD to assume the S-shaped structure, where the O−H···F hydrogen bond is replaced by another O−H···O hydrogen bond, which is energetically more favorable. As a consequence of this key-lock type interaction, checkerboard patterns (as shown in Figure 1) are preferred over striped phases. It is also expected to be favorable over phase separation, which has been reported occasionally for mixed layers.[60,61] Structures with a "wrongly oriented" hydrogen bond or with different arrangements are significantly higher in energy (about 0.15 eV/molecule, cf. Supporting Information). Hence, even at significantly increased temperatures they are thermally occupied only by a few percent. Hence, these higher-lying geometries are not expected to affect the properties of the system significantly.

In Figures 4a and 4b, we report the resulting min(γ) configuration in the form of a surface phase diagram on Cu(111) and Ag(111). It is important to bear in mind that the outlaid thermodynamic model just describes steady state conditions. We do not and cannot make statements about reaction mechanisms or rates or the time scale required to achieve equilibrium. In practice, to get sufficient yield from the chemical reaction, it may be necessary to activate hydrogen, e.g., through a tungsten filament or elevated temperature. Furthermore, at very high temperatures (above 500 K) the molecules might undergo chemical reactions, e.g., through dehalogenation, which we do not consider in this work. Also, note that since we employed a supercell containing a finite number of molecules f can only be varied in discrete steps. In reality, of course, a smooth, continuous change of the mixing would be expected.

For a Cu(111) surface (Figure 4a) we find that at room temperature (ca. 300 K) for hydrogen pressures up to approximately 1 Pa f = 50% is predicted. To achieve smaller f, H_2 pressures which are hardly attainable in UHV equipment (and much less under industrial conditions) would be required. We emphasize, however, that the ratio for a given (p, T) can be adjusted by modifying the relative stability of the molecules. This can be easily achieved through chemical modification: Electron-donating groups like methyl or hydroxyl groups stabilize the quinone form, whereas electron-accepting substituents such as halogens stabilize the diol form.[30] If necessary, it should, therefore, be possible to modify acenequinones such that the desired mixing ratio is in a more "convenient" pressure/temperature range.

For the TFBQ/TFBD system, our results in fact imply that pure acenequinone layers might be thermodynamically not stable at room temperature in UHV conditions, as they will eventually be reduced by residual hydrogen gas. This, however, does not exclude that such homogeneous layers are metastable, as the reaction with hydrogen involves a reaction barrier. Thus, they likely exist over a considerable time scale. Increasing the hydrogen pressure to medium vacuum conditions (>1 Pa) the equilibrium TFBD fraction can be continuously changed up to f = 100%. At elevated temperature, e.g., at 450 K, almost any mixing ratio, including f = 0%, can be achieved with p_{H2} ranging from UHV to atmospheric pressure.

On Ag(111), due to the lower reactivity of the surface, configurations with larger TFBD fractions become stabilized compared to adsorption on Cu(111). Consequently, the transition lines from f = 25% to 50% and f = 50% to 75% shift to higher temperatures and hydrogen pressures.

Work-Function Modifications As a Function of Coverage and Mixing Ratio. Having established that, in principle, arbitrary values of f can be obtained by controlling the substrate temperature and the H_2 partial pressure, the logical next step is to investigate how $\Delta\Phi$ depends on f. At this point it is also useful to study how this compares to the situation of changing the coverage (θ) of a single compound. In the following we focus on the discussion on the electronic properties of the system; the impact of mixing on geometric properties, in

DOI: 10.1021/acs.jpcc.5b08827
J. Phys. Chem. C 2015, 119, 27162−27172

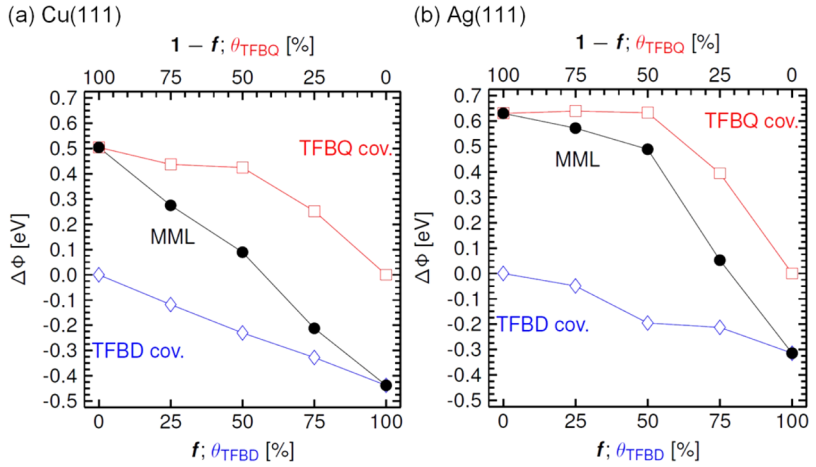

Figure 5. Work function modification ΔΦ for mixed monolayers of TFBQ and TFBD (black circles) with increasing TFBD fraction *f* for adsorption on (a) Cu(111) and (b) Ag(111). For comparison (see text) ΔΦ is also plotted for submonolayers of TFBQ (red squares) and TFBD (blue diamonds) as a function of coverage θ.

particular the mutual impact on the respective adsorption distances, is described in the Supporting Information.

We start the discussion with the adsorption of TFBD, which is the conceptually simpler system. The evolution of ΔΦ with coverage is shown by blue diamonds in Figures 5a (Cu) and in 5b (Ag). As mentioned before, here ΔΦ originates from a bond dipole caused by Pauli pushback, plus the molecular dipole. The magnitude of a pushback dipole depends mainly on the relative polarizabilities of substrate and adsorbate,[62] neither of which is significantly dependent on the molecular coverage. Hence, every molecule induces basically the same dipole with only a very small depolarization; similar effects, though with much larger depolarization, are also observed for the coverage dependence of dipolar self-assembled monolayers.[63,64] This results in a nearly linear $\Delta\Phi(\theta_{TFBD})$ dependency (blue diamonds). The apparent unsteadiness of the evolution originates from minor changes in the adsorption structures of TFBD at lower coverage. This modifies ΔE_{mol}, which is then reflected in the ΔΦ; ΔE_{bond} per molecule stays approximately constant.

For TFBQ, ΔΦ remains essentially constant on both substrates for coverages down to 50% (see red squares in Figure 5a and 5b). A significant decrease is found only at smaller θ_{TFBQ}. The region of constant ΔΦ may seem surprising at first: considering that the density of acceptors per area (θ_{TFBQ}) decreases, this implies that the dipole moment per TFBQ molecule increases. It is, however, exactly what one would expect for a Fermi-level pinned situation, where the dipole needs to be sufficiently large to shift the LUMO-derived band into resonance with the Fermi energy (i.e., where the level alignment determines the dipole, rather than *vice versa*).[38] This should stabilize the work function in an energy range determined by the width of the LUMO-derived peak of the DOS. For TFBQ on both metals at coverages between 100% and 50%, this expectation approximately holds. Conversely, for coverages below 50% the picture portrayed above collapses, and the aforementioned, pronounced decrease of ΔΦ sets in. Naively, one might expect that this is accompanied by a similarly large shift of the LUMO peak relative to the Fermi energy. Interestingly, this is not the case. As shown in Figure 6, between θ = 100% and θ = 25% the LUMO peak shifts only by approximately 28 meV on Cu and approximately 13 meV on Ag (compared to a change in ΔΦ by more than 500 meV).

Rather, the reduction of ΔΦ originates from the inhomogeneity of the electrostatic energy above the surface. Before we explain in detail how this affects the current system, it is, once again, useful to illustrate two limiting cases.

If the adsorbate were a densely packed, perfectly homogeneous material (preferably without atomic structure), also charge would be evenly distributed. Adsorbate and molecule would correspond to a charged plate each. For this situation, the effect on the electrostatic energy, *U*, is well-known and shown as a red line in Figure 7a: *U* is flat below the first plate, increases linearly between the two plates, and becomes flat again directly above the second plate. In this picture, the difference in *U* above and below the plates would correspond to ΔΦ. Conversely, the most inhomogeneous situation would be realized if the adsorbate was a single point charge above the surface. This, too, is a textbook problem, and the effect on the electrostatic energy is shown as a blue dashed line in Figure 7a. *U* goes through singularities at the positions of the point charges. Away from the point charges *U* decays slowly, eventually reaching the same value both above and below the charged moieties. There is, in other words, no ΔΦ for this model system.

Naturally, any realistic system is between these two model notions. How quickly the electrostatic energy above an array of dipoles decays (i.e., how fast a constant vacuum level is reached) depends sensitively on the dipole spacing.[65] To illustrate how inhomogeneity pertains to the (sub-)monolayers of TFBQ, we have calculated the adsorption-induced, plane-averaged electrostatic energy rearrangements ΔU upon adsorption of the organic material

$$\Delta U(z) = \frac{1}{A}\iint_{\text{ads. site of TFBQ}} [U_{sys}(\vec{r}) - U_{slab}(\vec{r}) - U_{fsm}(\vec{r})]\,dx\,dy \quad (8)$$

Here *A* is the area of a single adsorption site, U_{sys} the electrostatic energy of the combined system, U_{slab} the electrostatic energy of the metal without the adsorbed layer, and U_{fsm} the electrostatic energy of the free-standing monolayer without the metal. For the homogeneous monolayer of TFBQ the results are shown in Figure 7b (Cu) and Figure 7c (Ag) as solid red lines. There, we find that no field above the layer is present, and the evolution of the electrostatic energy closely

DOI: 10.1021/acs.jpcc.5b08827
J. Phys. Chem. C 2015, 119, 27162−27172

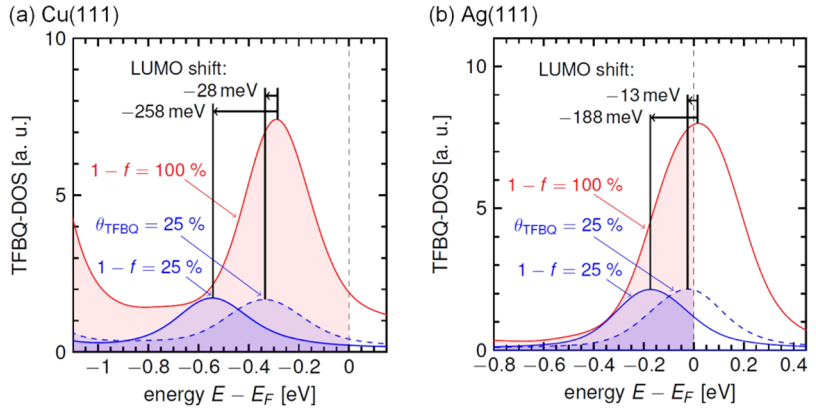

Figure 6. Comparison of the density of states for a TFBQ monolayer with θ = 100% (red line) and θ = 25% (blue, dashed line) and for a mixed monolayer with $1 - f$ = 25% (blue line) adsorbed upon (a) Cu(111) and (b) Ag(111). The black arrows indicate the shift of the LUMO peak.

resembles the case of a plate capacitor. As a result, the states in the molecular layer are shifted by approximately the same energy as the vacuum level relative to the Fermi energy of the metal.

The situation changes markedly for submonolayers of TFBQ with θ_{TFBQ} = 25% (blue, dashed lines in Figure 7b and 7c): ΔU shows a pronounced decrease above the location of the molecule. The situation is thus more reminiscent of the point charge notion, although a finite $\Delta\Phi$ remains. An important feature here is that, relative to the Fermi energy, the states of the molecule are shifted *more* than the vacuum level. This explains the aforementioned observation that below a certain coverage $\Delta\Phi$ and the energy of the LUMO do not directly correlate with each other any more.

For mixed monolayers of TFBQ and TFBD (black circles in Figure 5), we find that $\Delta\Phi$ correlates strongly with f, indicating that changing the mixing ratio of these two molecules provides a sensible leverage to tune the work function. This could not have been the case if $\Delta\Phi$ was determined exclusively by the Fermi-level pinned part of the system (TFBQ). The presence of TFBD modifies level alignment and $\Delta\Phi$ in two ways compared to the submonolayer coverage situation.

The presence of the donor (TFBD) decreases the electrostatic energy at the position of the acceptor (TFBQ), as discussed by Rissner at al. for the case of mixed thiolate-bonded monolayers of upright-standing molecules.[27] As Figure 7b and 7c shows (blue, solid line), ΔU at z = 0 Å is smaller for the mixed monolayer than for the submonolayer coverage. As a result, the TFBQ-LUMO is shifted to lower energies relative to E_F (as is also evident from Figure 6). This results in a larger net charge transfer from the metal to TFBQ.

Although the effect on the electrostatic energy at the position of the molecule explains the level alignment, it does not suffice to explain why the work function differs between the submonolayer and mixed layer cases nor why the difference between these cases is so much larger on Cu than on Ag. To explain these differences, it is necessary to recall that TFBD adsorbs at a larger distance than TFBQ. As we have shown previously for the case of molecular dipoles,[66] in Fermi-level pinned systems any shift of the electrostatic energy that is introduced between the metal and the TFBQ layer will be compensated by a modification of the charge transfer to the LUMO (in agreement with Figure 6). Thus, it does not affect $\Delta\Phi$; a more detailed discussion of this situation is provided in the Supporting Information. Conversely, shifts that are located above the molecular backbone do have an immediate effect on $\Delta\Phi$. Hence, when compared to the submonolayer situation, TFBD affects the net $\Delta\Phi$ more the larger the distance between TFBQ and TFBD is. Although in mixing cases the adsorption distances of donor and acceptor are known to become more similar,[67] they never become equal, and their difference always remains much larger on Cu than on Ag (by approximately 0.4 Å). As a consequence, the $\Delta\Phi$ evolution for mixed monolayers follows the submonolayer evolution much more closely on Ag than on Cu.

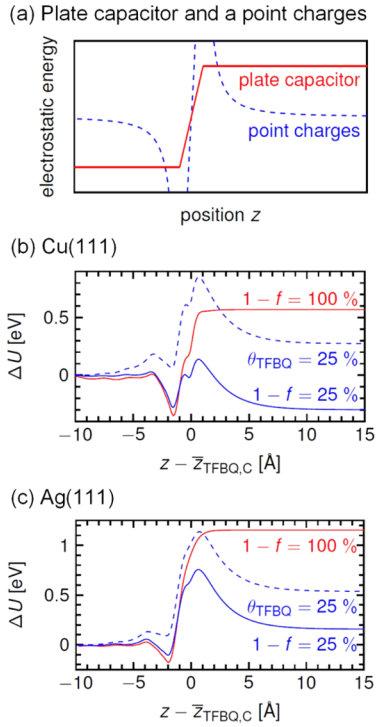

Figure 7. (a) Sketch of the plane-averaged electrostatic energy distribution for two charged plates (red) vs two point charges (blue). Rearrangements of the electrostatic energy ΔU due to adsorption of TFBQ monolayers with θ = 100% (red line) and θ = 25% (blue, dashed line) and for a mixed monolayer with $1 - f$ = 25% (blue line) on (b) Cu(111) and (c) Ag(111). The origins of the abscissa and the ordinate are aligned to the mean position of the carbon atoms of TFBQ and to the vacuum level below the slab.

DOI: 10.1021/acs.jpcc.5b08827
J. Phys. Chem. C 2015, 119, 27162−27172

4. CONCLUSION

We employed density functional theory coupled with *ab initio* thermodynamics to demonstrate the possibility of tuning coinage metal work functions through adsorption of a donor−acceptor pair that is coupled via a redox reaction. Our investigations show that the mixing ratio and, thus, the substrate work function can be adjusted postadsorption by exerting control over the pressure of a surrounding H_2 gas. For the example of the TFBD/TFBQ pair we show that for temperatures between 300 and 500 K and at hydrogen pressures attainable from low to ultrahigh vacuum conditions the molecular species can be converted into each other quantitatively. This allows changing the work function over a range of approximately 1 eV on both Cu(111) and Ag(111). We anticipate that the discussed mechanism, i.e., exploiting surface reactions to tune the work function after deposition of the organic material, may help in producing substrates with more reproducible work functions and, thus, charge injection barriers.

Furthermore, we studied how the work function and the level alignment differ between the mixed layers and submonolayer coverages. We showed that for understanding both mixed monolayers and incomplete coverage adsorbate layers the commonly applied concept of Fermi-level pinning for charge-transfer monolayers has to be significantly extended to account for inhomogeneities of the fields at the surface.

■ ASSOCIATED CONTENT

Supporting Information

The Supporting Information is available free of charge on the ACS Publications website at DOI: 10.1021/acs.jpcc.5b08827.

Information about supercell geometries, bond dipole and molecular dipole evolutions for submonolayers of TFBD adsorbed upon Ag(111), as well as adsorption heights, Mulliken charges, a detailed model for the level alignment in mixed monolayers, IR spectra of TFBQ and TFBD, a short discussion of extraction effects of metal atoms due to TFBQ adsorption, and molecular orbital projected density of states for TFBQ adsorbed on Cu(111) and Ag(111) (PDF)

■ AUTHOR INFORMATION

Corresponding Author

*Tel.: +43 316 873 8465. Fax: +43 316 873 8466. E-mail: o.hofmann@tugraz.at.

Author Contributions

The manuscript was written through contributions of all authors. All authors have given approval to the final version of the manuscript.

Notes

The authors declare no competing financial interest.

■ ACKNOWLEDGMENTS

We thank Philipp Herrmann, Georg Heimel, and Shashank S. Harivyasi for helpful discussions and Björn Bieniek for his help with the implementation of the output of the Hartree potential. The computational results presented have been achieved in part using the Vienna Scientific Cluster (VSC). Funding by the Austrian Science Fund (FWF) through the Erwin-Schrödinger Grant No. J 3285-N20 and by the EU Marie Curie Actions ITN THINFACE (FP7/2007-2013/607232) is gratefully acknowledged.

■ REFERENCES

(1) Koch, N. Organic Electronic Devices and Their Functional Interfaces. *ChemPhysChem* **2007**, *8* (10), 1438−1455.

(2) Peng, Y.-Q.; Lu, F.-P. Injection of Holes at Indium Tin Oxide/dendrimer Interface: An Explanation with New Theory of Thermionic Emission at Metal/organic Interfaces. *Appl. Surf. Sci.* **2006**, *252* (18), 6275−6279.

(3) Gruber, M.; Zojer, E.; Schürrer, F.; Zojer, K. Impact of Materials versus Geometric Parameters on the Contact Resistance in Organic Thin-Film Transistors. *Adv. Funct. Mater.* **2013**, *23* (23), 2941−2952.

(4) Le, Q. T.; Yan, L.; Gao, Y.; Mason, M. G.; Giesen, D. J.; Tang, C. W. Photoemission Study of Aluminum/tris-(8-Hydroxyquinoline) Aluminum and aluminum/LiF/tris-(8-Hydroxyquinoline) Aluminum Interfaces. *J. Appl. Phys.* **2000**, *87* (1), 375.

(5) Chan, M. Y.; Lai, S. L.; Fung, M. K.; Tong, S. W.; Lee, C. S.; Lee, S. T. Efficient CsF/Yb/Ag Cathodes for Organic Light-Emitting Devices. *Appl. Phys. Lett.* **2003**, *82* (11), 1784.

(6) Gossenberger, F.; Roman, T.; Forster-Tonigold, K.; Groß, A. Change of the Work Function of Platinum Electrodes Induced by Halide Adsorption. *Beilstein J. Nanotechnol.* **2014**, *5*, 152−161.

(7) Cao, Y.; Yu, G.; Parker, I. D.; Heeger, A. J. Ultrathin Layer Alkaline Earth Metals as Stable Electron-Injecting Electrodes for Polymer Light Emitting Diodes. *J. Appl. Phys.* **2000**, *88* (6), 3618.

(8) Nakamura, A.; Tada, T.; Mizukami, M.; Yagyu, S. Efficient Electrophosphorescent Polymer Light-Emitting Devices Using a Cs/Al Cathode. *Appl. Phys. Lett.* **2004**, *84* (1), 130.

(9) Chou, S. H.; Voss, J.; Vojvodic, A.; Howe, R. T.; Abild-Pedersen, F. DFT Study of Atomically-Modified Alkali-Earth Metal Oxide Films on Tungsten. *J. Phys. Chem. C* **2014**, *118* (21), 11303−11309.

(10) Giordano, L.; Cinquini, F.; Pacchioni, G. Tuning the Surface Metal Work Function by Deposition of Ultrathin Oxide Films: Density Functional Calculations. *Phys. Rev. B: Condens. Matter Mater. Phys.* **2006**, DOI: 10.1103/PhysRevB.73.045414.

(11) de Boer, B.; Hadipour, A.; Mandoc, M. M.; van Woudenbergh, T.; Blom, P. W. M. Tuning of Metal Work Functions with Self-Assembled Monolayers. *Adv. Mater.* **2005**, *17* (5), 621−625.

(12) Campbell, I.; Rubin, S.; Zawodzinski, T.; Kress, J.; Martin, R.; Smith, D.; Barashkov, N.; Ferraris, J. Controlling Schottky Energy Barriers in Organic Electronic Devices Using Self-Assembled Monolayers. *Phys. Rev. B: Condens. Matter Mater. Phys.* **1996**, *54* (20), R14321−R14324.

(13) Zehner, R. W.; Parsons, B. F.; Hsung, R. P.; Sita, L. R. Tuning the Work Function of Gold with Self-Assembled Monolayers Derived from $X-[C_6H_4-C{\vdots}C-]_nC_6H_4-SH$ (n = 0, 1, 2; X = H, F, CH_3, CF_3, and OCH_3). *Langmuir* **1999**, *15* (4), 1121−1127.

(14) Zuppiroli, L.; Si-Ahmed, L.; Kamaras, K.; Nüesch, F.; Bussac, M. N.; Ades, D.; Siove, A.; Moons, E.; Grätzel, M. Self-Assembled Monolayers as Interfaces for Organic Opto-Electronic Devices. *Eur. Phys. J. B* **1999**, *11* (3), 505−512.

(15) Yan, H.; Huang, Q.; Cui, J.; Veinot, J. G. C.; Kern, M. M.; Marks, T. J. High-Brightness Blue Light-Emitting Polymer Diodes via Anode Modification Using a Self-Assembled Monolayer. *Adv. Mater.* **2003**, *15* (10), 835−838.

(16) Bock, C.; Pham, D. V.; Kunze, U.; Käfer, D.; Witte, G.; Wöll, C. Improved Morphology and Charge Carrier Injection in Pentacene Field-Effect Transistors with Thiol-Treated Electrodes. *J. Appl. Phys.* **2006**, *100* (11), 114517.

(17) Romaner, L.; Heimel, G.; Brédas, J.-L.; Gerlach, A.; Schreiber, F.; Johnson, R.; Zegenhagen, J.; Duhm, S.; Koch, N.; Zojer, E. Impact of Bidirectional Charge Transfer and Molecular Distortions on the Electronic Structure of a Metal-Organic Interface. *Phys. Rev. Lett.* **2007**, DOI: 10.1103/PhysRevLett.99.256801.

(18) Duhm, S.; Glowatzki, H.; Cimpeanu, V.; Klankermayer, J.; Rabe, J. P.; Johnson, R. L.; Koch, N. Weak Charge Transfer between an

Acceptor Molecule and Metal Surfaces Enabling Organic/Metal Energy Level Tuning. *J. Phys. Chem. B* **2006**, *110* (42), 21069−21072.
(19) Stadtmüller, B.; Kröger, I.; Reinert, F.; Kumpf, C. Submonolayer Growth of CuPc on Noble Metal Surfaces. *Phys. Rev. B: Condens. Matter Mater. Phys.* **2011**, DOI: 10.1103/PhysRevB.83.085416.
(20) Koch, N.; Duhm, S.; Rabe, J. P.; Rentenberger, S.; Johnson, R. L.; Klankermayer, J.; Schreiber, F. Tuning the Hole Injection Barrier Height at Organic/metal Interfaces with (sub-) Monolayers of Electron Acceptor Molecules. *Appl. Phys. Lett.* **2005**, *87* (10), 101905.
(21) Rana, O.; Srivastava, R.; Chauhan, G.; Zulfequar, M.; Husain, M.; Srivastava, P. C.; Kamalasanan, M. N. Modification of Metal-Organic Interface Using F_4-TCNQ for Enhanced Hole Injection Properties in Optoelectronic Devices. *Phys. Status Solidi A* **2012**, *209* (12), 2539−2545.
(22) Ilyas, N.; Monti, O. L. A. Interplay of Local and Global Interfacial Electronic Structure of a Strongly Coupled Dipolar Organic Semiconductor. *Phys. Rev. B: Condens. Matter Mater. Phys.* **2014**, DOI: 10.1103/PhysRevB.90.125435.
(23) Bröker, B.; Hofmann, O. T.; Rangger, G. M.; Frank, P.; Blum, R.-P.; Rieger, R.; Venema, L.; Vollmer, A.; Müllen, K.; Rabe, J. P. Density-Dependent Reorientation and Rehybridization of Chemisorbed Conjugated Molecules for Controlling Interface Electronic Structure. *Phys. Rev. Lett.* **2010**, DOI: 10.1103/PhysRevLett.104.246805.
(24) Kilian, L.; Umbach, E.; Sokolowski, M. Molecular Beam Epitaxy of Organic Films Investigated by High Resolution Low Energy Electron Diffraction (SPA-LEED): 3,4,9,10-Perylenetetracarboxylica-cid-Dianhydride (PTCDA) on Ag(111). *Surf. Sci.* **2004**, *573* (3), 359−378.
(25) Tautz, F. S. Structure and Bonding of Large Aromatic Molecules on Noble Metal Surfaces: The Example of PTCDA. *Prog. Surf. Sci.* **2007**, *82* (9−12), 479−520.
(26) Teichert, C.; Hlawacek, G.; Andreev, A. Y.; Sitter, H.; Frank, P.; Winkler, A.; Sariciftci, N. S. Spontaneous Rearrangement of Para-Sexiphenyl Crystallites into Nano-Fibers. *Appl. Phys. A: Mater. Sci. Process.* **2006**, *82* (4), 665−669.
(27) Rissner, F.; Egger, D. A.; Romaner, L.; Heimel, G.; Zojer, E. The Electronic Structure of Mixed Self-Assembled Monolayers. *ACS Nano* **2010**, *4* (11), 6735−6746.
(28) Wu, K.-Y.; Yu, S.-Y.; Tao, Y.-T. Continuous Modulation of Electrode Work Function with Mixed Self-Assembled Monolayers and Its Effect in Charge Injection. *Langmuir* **2009**, *25* (11), 6232−6238.
(29) We note that a similar approach should also work for deposition from solution, where the mixing ratio could be adjusted via its pH value.
(30) Streitwieser, A.; Heathcock, C. H.; Kosower, E. M. *Organische Chemie*; VCH: Weinheim [u.a.], 1994.
(31) Marder, S. R.; Kippelen, B.; Jen, A. K.-Y.; Peyghambarian, N. Design and Synthesis of Chromophores and Polymers for Electro-Optic and Photorefractive Applications. *Nature* **1997**, *388* (6645), 845−851.
(32) Heimel, G.; Duhm, S.; Salzmann, I.; Gerlach, A.; Strozecka, A.; Niederhausen, J.; Bürker, C.; Hosokai, T.; Fernandez-Torrente, I.; Schulze, G.; et al. Charged and Metallic Molecular Monolayers through Surface-Induced Aromatic Stabilization. *Nat. Chem.* **2013**, *5* (3), 187−194.
(33) Blum, V.; Gehrke, R.; Hanke, F.; Havu, P.; Havu, V.; Ren, X.; Reuter, K.; Scheffler, M. Ab Initio Molecular Simulations with Numeric Atom-Centered Orbitals. *Comput. Phys. Commun.* **2009**, *180* (11), 2175−2196.
(34) Perdew, J. P.; Burke, K.; Ernzerhof, M. Generalized Gradient Approximation Made Simple. *Phys. Rev. Lett.* **1996**, *77* (18), 3865−3868.
(35) We have also performed calculations using the PW91-functional. Only minor quantitative changes were found.
(36) Ruiz, V. G.; Liu, W.; Zojer, E.; Scheffler, M.; Tkatchenko, A. Density-Functional Theory with Screened van Der Waals Interactions for the Modeling of Hybrid Inorganic-Organic Systems. *Phys. Rev. Lett.* **2012**, DOI: 10.1103/PhysRevLett.108.146103.
(37) For the sake of consistency, we have also performed calculations using the PW91-functional.
(38) Hofmann, O. T.; Atalla, V.; Moll, N.; Rinke, P.; Scheffler, M. Interface Dipoles of Organic Molecules on Ag(111) in Hybrid Density-Functional Theory. *New J. Phys.* **2013**, *15* (12), 123028.
(39) Ferri, N.; DiStasio, R. A.; Ambrosetti, A.; Car, R.; Tkatchenko, A. Electronic Properties of Molecules and Surfaces with a Self-Consistent Interatomic van Der Waals Density Functional. *Phys. Rev. Lett.* **2015**, DOI: 10.1103/PhysRevLett.114.176802.
(40) Freysoldt, C.; Eggert, P.; Rinke, P.; Schindlmayr, A.; Scheffler, M. Screening in Two Dimensions: G W Calculations for Surfaces and Thin Films Using the Repeated-Slab Approach. *Phys. Rev. B: Condens. Matter Mater. Phys.* **2008**, DOI: 10.1103/PhysRevB.77.235428.
(41) Paier, J.; Marsman, M.; Kresse, G. Why Does the B3LYP Hybrid Functional Fail for Metals? *J. Chem. Phys.* **2007**, *127* (2), 024103.
(42) Monkhorst, H. J.; Pack, J. D. Special Points for Brillouin-Zone Integrations. *Phys. Rev. B* **1976**, *13* (12), 5188−5192.
(43) Lu, F.; Salaita, G. N.; Laguren-Davidson, L.; Stern, D. A.; Wellner, E.; Frank, D. G.; Batina, N.; Zapien, D. C.; Walton, N.; Hubbard, A. T. Characterization of Hydroquinone and Related Compounds Adsorbed at Pt(111) from Aqueous Solutions: Electron Energy-Loss Spectroscopy, Auger Spectroscopy, LEED, and Cyclic Voltammetry. *Langmuir* **1988**, *4* (3), 637−646.
(44) Kim, Y.-G.; Baricuatro, J. H.; Soriaga, M. P. Molecular Adsorption at Well-Defined Electrode Surfaces: Hydroquinone on Pd(111) Studied by EC-STM †. *Langmuir* **2006**, *22* (25), 10762−10765.
(45) Inukai, J.; Wakisaka, M.; Yamagishi, M.; Itaya, K. Adlayer of Hydroquinone on Rh(111) in Solution and in Vacuum Studied by STM and LEED. *J. Electrochem. Soc.* **2005**, *152* (2), E35.
(46) Reuter, K.; Scheffler, M. Composition, Structure, and Stability of RuO2(110) as a Function of Oxygen Pressure. *Phys. Rev. B: Condens. Matter Mater. Phys.* **2001**, DOI: 10.1103/PhysRevB.65.035406.
(47) Herrmann, P.; Heimel, G. Structure and Stoichiometry Prediction of Surfaces Reacting with Multicomponent Gases. *Adv. Mater.* **2015**, *27* (2), 255−260.
(48) Rogal, J.; Reuter, K. Ab Initio Atomistic Thermodynamics for Surfaces: A Primer. 2007, *Neuilly-sur-Seine* (Educational Notes RTO-EN-AVT-142); p 2-1−2-18.
(49) Loffreda, D. Theoretical Insight of Adsorption Thermodynamics of Multifunctional Molecules on Metal Surfaces. *Surf. Sci.* **2006**, *600* (10), 2103−2112.
(50) Nolting, W.; Nolting, W. *Statistische Physik: mit 133 Aufgaben mit vollständigen Lösungen*, 6. Aufl.; Grundkurs Theoretische Physik; Springer: Berlin, 2007.
(51) Duhm, S.; Gerlach, A.; Salzmann, I.; Bröker, B.; Johnson, R. L.; Schreiber, F.; Koch, N. PTCDA on Au(111), Ag(111) and Cu(111): Correlation of Interface Charge Transfer to Bonding Distance. *Org. Electron.* **2008**, *9* (1), 111−118.
(52) Koch, N.; Gerlach, A.; Duhm, S.; Glowatzki, H.; Heimel, G.; Vollmer, A.; Sakamoto, Y.; Suzuki, T.; Zegenhagen, J.; Rabe, J. P.; et al. Adsorption-Induced Intramolecular Dipole: Correlating Molecular Conformation and Interface Electronic Structure. *J. Am. Chem. Soc.* **2008**, *130* (23), 7300−7304.
(53) Bagus, P.; Staemmler, V.; Wöll, C. Exchangelike Effects for Closed-Shell Adsorbates: Interface Dipole and Work Function. *Phys. Rev. Lett.* **2002**, DOI: 10.1103/PhysRevLett.89.096104.
(54) Hofmann, O. T.; Rangger, G. M.; Zojer, E. Reducing the Metal Work Function beyond Pauli Pushback: A Computational Investigation of Tetrathiafulvalene and Viologen on Coinage Metal Surfaces. *J. Phys. Chem. C* **2008**, *112* (51), 20357−20365.
(55) Ito, E.; Oji, H.; Ishii, H.; Oichi, K.; Ouchi, Y.; Seki, K. Interfacial Electronic Structure of Long-Chain Alkane/metal Systems Studied by UV-Photoelectron and Metastable Atom Electron Spectroscopies. *Chem. Phys. Lett.* **1998**, *287* (1−2), 137−142.
(56) Heimel, G.; Rissner, F.; Zojer, E. Modeling the Electronic Properties of π-Conjugated Self-Assembled Monolayers. *Adv. Mater.* **2010**, *22* (23), 2494−2513.

DOI: 10.1021/acs.jpcc.5b08827
J. Phys. Chem. C 2015, 119, 27162−27172

(57) Romaner, L.; Nabok, D.; Puschnig, P.; Zojer, E.; Ambrosch-Draxl, C. Theoretical Study of PTCDA Adsorbed on the Coinage Metal Surfaces, Ag(111), Au(111) and Cu(111). *New J. Phys.* **2009**, *11* (5), 053010.
(58) Ditze, S.; Stark, M.; Buchner, F.; Aichert, A.; Jux, N.; Luckas, N.; Görling, A.; Hieringer, W.; Hornegger, J.; Steinrück, H.-P.; et al. On the Energetics of Conformational Switching of Molecules at and Close to Room Temperature. *J. Am. Chem. Soc.* **2014**, *136* (4), 1609−1616.
(59) Mercurio, G.; Maurer, R. J.; Liu, W.; Hagen, S.; Leyssner, F.; Tegeder, P.; Meyer, J.; Tkatchenko, A.; Soubatch, S.; Reuter, K. Quantification of Finite-Temperature Effects on Adsorption Geometries of π -Conjugated Molecules: Azobenzene/Ag(111). *Phys. Rev. B: Condens. Matter Mater. Phys.* **2013**, DOI: 10.1103/PhysRevB.88.035421.
(60) Otero, R.; Écija, D.; Fernández, G.; Gallego, J. M.; Sánchez, L.; Martín, N.; Miranda, R. An Organic Donor/Acceptor Lateral Superlattice at the Nanoscale. *Nano Lett.* **2007**, *7* (9), 2602−2607.
(61) Stranick, S. J.; Parikh, A. N.; Tao, Y.-T.; Allara, D. L.; Weiss, P. S. Phase Separation of Mixed-Composition Self-Assembled Monolayers into Nanometer Scale Molecular Domains. *J. Phys. Chem.* **1994**, *98* (31), 7636−7646.
(62) Bagus, P. S.; Käfer, D.; Witte, G.; Wöll, C. Work Function Changes Induced by Charged Adsorbates: Origin of the Polarity Asymmetry. *Phys. Rev. Lett.* **2008**, DOI: 10.1103/PhysRevLett.100.126101.
(63) Monti, O. L. A. Understanding Interfacial Electronic Structure and Charge Transfer: An Electrostatic Perspective. *J. Phys. Chem. Lett.* **2012**, *3* (17), 2342−2351.
(64) Romaner, L.; Heimel, G.; Zojer, E. Electronic Structure of Thiol-Bonded Self-Assembled Monolayers: Impact of Coverage. *Phys. Rev. B: Condens. Matter Mater. Phys.* **2008**, DOI: 10.1103/PhysRevB.77.045113.
(65) Natan, A.; Kronik, L.; Haick, H.; Tung, R. T. Electrostatic Properties of Ideal and Non-Ideal Polar Organic Monolayers: Implications for Electronic Devices. *Adv. Mater.* **2007**, *19* (23), 4103−4117.
(66) Hofmann, O. T.; Egger, D. A.; Zojer, E. Work-Function Modification beyond Pinning: When Do Molecular Dipoles Count? *Nano Lett.* **2010**, *10* (11), 4369−4374.
(67) Stadtmüller, B.; Lüftner, D.; Willenbockel, M.; Reinisch, E. M.; Sueyoshi, T.; Koller, G.; Soubatch, S.; Ramsey, M. G.; Puschnig, P.; Tautz, F. S. Unexpected Interplay of Bonding Height and Energy Level Alignment at Heteromolecular Hybrid Interfaces. *Nat. Commun.* **2014**, DOI: 10.1038/ncomms4685.

DOI: 10.1021/acs.jpcc.5b08827
J. Phys. Chem. C 2015, 119, 27162−27172